Bioorganic Chemistry 38 (2010) 7–16

Contents lists available at ScienceDirect

Bioorganic Chemistry

journal homepage: www.elsevier.com/locate/bioorg

Electronic circular dichroism of monomethyl [^{16}O, ^{17}O, ^{18}O]-phosphate and [^{16}O, ^{17}O, ^{18}O]-thiophosphate revisited

Jian-Jung Pan, Boris A. Kashemirov, Joanne Lee, Charles E. McKenna *, Frank J. Devlin, Philip J. Stephens *

Department of Chemistry, University of Southern California, Los Angeles, CA 90089, USA

ARTICLE INFO

Article history:
Received 7 July 2007
Available online 25 February 2009

Keywords:
Phosphoryl-transfer
Isotopically-chiral phosphates
Electronic circular dichroism

ABSTRACT

Phosphoryl-transfer reactions have long been of interest due to their importance in maintaining numerous cellular functions. A phosphoryl-transfer reaction results in two possible stereochemical outcomes: either retention or inversion of configuration at the transferred phosphorus atom. When the product is phosphate, isotopically-labeled [^{16}O, ^{17}O, ^{18}O]-phosphate derivatives can be used to distinguish these outcomes; one oxygen must be replaced by sulfur or esterified to achieve isotopic chirality. Conventionally, stereochemical analysis of isotopically chiral phosphate has been based on ^{31}P NMR spectroscopy and involves complex chemical or enzymatic transformations. An attractive alternative would be direct determination of the enantiomeric excess using chiroptical spectroscopy. (*S*)-Methyl-[^{16}O, ^{17}O, ^{18}O]-phosphate (MePi*), **7** and enantiomeric [^{16}O, ^{17}O, ^{18}O]-thiophosphate (TPi*), **10**, were previously reported to exhibit weak electronic circular dichroism (ECD), although with **10** the result was considered to be uncertain. We have now re-examined the possibility that excesses of **7** and **10** enantiomers can be detected by ECD spectrometry, using both experimental and theoretical approaches. **7** and both the (*R*) and (*S*) enantiomers of **10** (**10a**, **10b**) were synthesized by the 'Oxford route' and characterized by ^{1}H, ^{31}P and ^{17}O NMR, and by MS analysis. Weak ECD could be found for **7**, with suboptimal S/N. No significant ECD could be detected for the **10** enantiomers.

Time-dependent DFT (TDDFT) calculations of the electronic excitation energies and rotational strengths of the same three enantiomers were carried out using the functional B3LYP and the basis set 6-311G**. The isotopically-perturbed geometries were predicted using the anharmonic vibrational frequency calculational code in GAUSSIAN 03. In the case of **10**, calculations were also carried out for the hexahydrated complex to investigate the influence of the aqueous solvent. The predicted excitation wavelengths are greater than the observed wavelengths, a not unusual result of TDDFT calculations. The predicted anisotropy ratios are 2.9×10^{-5} for **7**, -5.3×10^{-6} for **10a/b**, and 1.7×10^{-6} for **10a/b**·$(H_2O)_6$. For **7** the predicted anisotropy ratio approximates that observed in this work, 4.5×10^{-5} at 208 nm. For **10a/b**, the upper limits of the experimental anisotropy ratios ($<5 \times 10^{-6}$ at 225 nm, pH 9; $<5 \times 10^{-6}$ at 236 nm, pH 12) are comparable to the predicted magnitude of the value for **10a/b**. The lower predicted value for **10a/b** · $(H_2O)_6$ suggests that the aqueous environment affects the ECD significantly. Altogether, the TDDFT calculations together with a stereochemical analysis based on NMR and the MS data support the conclusion that the experimental ECD results for MePi* and TPi* may be reliable in order of magnitude.

1. Introduction

Phosphoryl-transfer reactions have long been of interest due to their importance in maintaining numerous cellular functions, such as reversible phosphorylation by kinases/phosphatases [1–3]. Abnormal regulation of phosphorylation often leads to numerous diseases [4–6]. As a result, these enzymes are potential targets for rational drug design [7,8]. Despite efforts over several decades to understand phosphoryl-transfer reactions, their mechanisms are still being debated [9–11]. A particular phosphoryl-transfer reaction could proceed by one of three mechanistically distinguishable pathways: concerted, associative or dissociative, as illustrated in Fig. 1. In the concerted pathway, the attacking nucleophile group forms a partial bond to the phosphorus atom simultaneously with partial dissociation of the leaving group, forming a high-energy transition state. In the associative pathway, both the attacking nucleophile and the leaving group reside in a local energy-minimum intermediate, i.e. a pentavalent phosphorane, in which they are singly bonded to the phosphorus atom. In the dissociative pathway, breaking of the leaving group bond to the phosphorus atom precedes bonding to the attacking nucleophile, resulting in a local

* Corresponding authors. Fax: +1 213 740 0930 (C.E. McKenna), +1 213 740 3972 (P.J. Stephens).
E-mail addresses: mckenna@usc.edu (C.E. McKenna), pstephen@usc.edu (P.J. Stephens).

0045-2068/$ - see front matter © 2010 Published by Elsevier Inc.
doi:10.1016/j.bioorg.2009.02.001

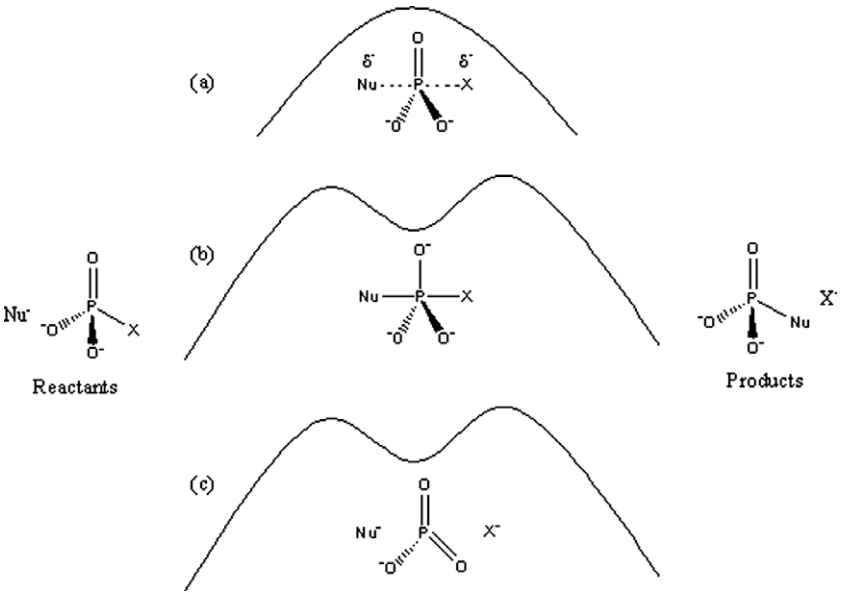

Fig. 1. The three mechanisms of a phosphoryl-transfer reaction: (a) concerted, (b) associative, (c) dissociative. The curved lines are hypothetical reaction free energy profiles. Nu: the nucleophile; X: the leaving group.

energy-minimum intermediate, i.e. a trivalent metaphosphate. These three mechanisms predict different stereochemical outcomes at phosphorus: respectively, (1) inversion, (2) inversion or retention (depending on the stability of the phosphorane intermediate), or (3) racemization, which may be only partial, again depending on the stability of the intermediate metaphosphate. Thus, the stereochemical fate of the transferred phosphate group is an important probe of the mechanism of the phosphoryl-transfer reaction. However, to confer chirality on the phosphorus atom with minimal structural perturbation is by no means trivial, because the obvious approach, isotopic substitution, is hindered by the availability of only three oxygen isotopes. Thus, the fourth oxygen must be replaced with sulfur, or else derivatized, for example to an ester [12–15], as shown in Fig. 2.

The second challenge is to elucidate the stereochemical outcome by analysis of the isotopically-labeled products. X-ray crystallography is unable to distinguish enantiomers of isotopically-labeled phosphates. Initially, stereochemical analysis of isotopically chiral phosphates was chiefly based on ^{31}P NMR spectroscopy of derivatives obtained after complex chemical [16–18] or enzymatic [19] transformations. The inherent sensitivity of these complicated methodologies is low, and may be lowered by loss of label and racemization. It was pointed out some three decades ago by Cullis and Lowe that a simpler, more straightforward and intrinsically chiral methodology, such as circular dichroism (CD), if available and effective, would thus be of considerable value [20]. These workers reported that the electronic CD (ECD) of monomethyl-[^{16}O, ^{17}O, ^{18}O]-phosphate (MePi*) is observable, yielding after correction for a ^{17}O enrichment of 44% a maximal anisotropy ratio $\Delta\varepsilon/\varepsilon = +1.1 \times 10^{-4}$ at 208 nm for the (*S*) enantiomer, **7**, and concluded that their finding established a convenient chiroptical method for determining the configuration of isotopically chiral phosphate [20]. However, in a subsequent review [13], Lowe characterized the observed ellipticity as being too small to have more than theoretical interest. Tsai reported an anisotropy ratio of similar magnitude (1.5×10^{-4} at 225 nm) for [^{16}O, ^{17}O, ^{18}O]-thiophosphate (TPi*) (without ECD data), but expressed doubt about the reliability and utility of this result, due to the weakness of the signal [21]. The ECD of these compounds has remained unexplored since these early publications.

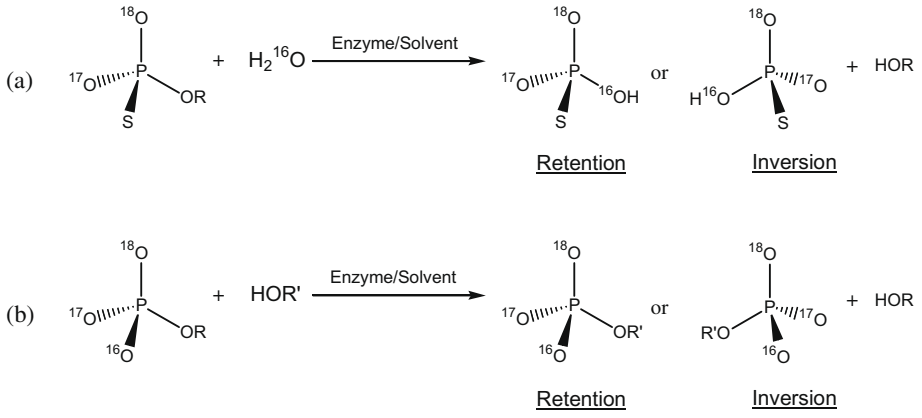

Fig. 2. The stereochemical outcomes of two isotopically-labeled phosphoryl-transfer reactions in the environments of the enzyme or solvent. The fourth oxygen of the products is replaced with (a) a sulfur atom or (b) an ester in order to make them chiral.

In this work, we re-evaluate the potential of ECD as a means to determine directly the absolute configurations of the isotopically-chiral phosphate compounds, using modern spectrometric and theoretical tools. We report details of the 'Oxford route' synthesis [18, 23] and improved purifications of MePi* and TPi*, more complete characterization data including ^{17}O NMR as well as MS data, and re-investigation of their ECD spectra.

2. Materials and methods

2.1. Materials

(*S*)-Mandelic acid (99%), phenyllithium (1.8 M in cyclohexane/ether, 70/30), monomethyl phosphate bis(cyclohexylammonium) salt, and sodium thiophosphate tribasic decahydrate were purchased from Aldrich. Anhydrous solvents (ethanol, pyridine, benzene, tetrahydrofuran (THF) and dioxane) were also purchased from Aldrich and used without further purification. $H_2{}^{18}O$ (^{16}O, 3.2%; ^{17}O, 2.2%; ^{18}O, 94.6%) and $H_2{}^{17}O$ (^{16}O, 52.4%; ^{17}O, 40.2%; ^{18}O, 7.4%) were purchased from ICON Isotopes.

2.2. Spectroscopy

2.2.1. General

^1H NMR spectra were recorded on either Bruker AM-360 or AC-250 MHz spectrometers and ^{31}P NMR spectra were recorded on the former. ^1H chemical shifts were referenced against TMS (δ_H 0.00) in $CDCl_3$ solution or HOD (δ_H 4.66) in D_2O solution, and ^{31}P against external 85% H_3PO_4 (δ_P 0.00). IR spectra were recorded on a Perkin Elmer 2000 FT-IR spectrometer. ECD spectra were obtained on a JASCO J-810 spectrometer at room temperature. UV spectra were measured on a Shimadzu UV-260. Preliminary UV spectroscopy on unlabeled TPi is documented in the Supplementary material. Negative ion FAB mass spectra were taken on a ZAB-ME spectrometer at the Analytical Chemistry Instrumentation Laboratory of the University of California, Riverside.

2.2.2. ^{17}O NMR of MePi*

^{17}O NMR spectra were recorded at 67.804 MHz on a Bruker AMX-500 NMR spectrometer. Inverse-gated decoupling was employed to obtain ^1H-decoupled NMR spectra without nuclear Overhauser effects (NOE). 600 transients were collected using 8192 data points with a spectral width (SW) of 50,000 Hz, a flip angle of 90° (PW = 8 μs), and an acquisition time (AQ) of 0.16389 s. A relaxation delay (RD) of 1 s was added between pulses resulting in a 1.163898 s recycle time. Chemical shifts were measured relative to naturally abundant $H_2{}^{17}O$ (δ_o = 0.0). Spectra were recorded at several different temperatures: room temperature (~300 K), 320, 345 and 365 K. The sample concentration was about 0.06 M in HPLC-grade water.

2.2.3. Mass spectrometric analysis of MePi* and TPi* samples

MS spectra of **7** and **10** were recorded in negative ion mode as the monoanions $[HO_2P(O)OCH_3]^-$and $[NaHO_2P(O)S]^-$, respectively. The statistical distribution of ions for each compound was calculated from the % enrichments of the $H_2{}^{18}O$ and $H_2{}^{17}O$ synthetic reagents, using an Apple iWork '09 Numbers spreadsheet. The RMS differences between the predicted and found peak intensities were minimized iteratively for three simple models: loss of ^{18}O, loss of ^{17}O, and loss of both labels. iMass 1.1 for Macintosh was used to construct the predicted spectra. Details including digitalized peak height data are given in the Supplementary material.

2.3. Synthesis

2.3.1. (S)-Benzoin **1**

(*S*)-Mandelic acid (4 g, 26 mmol) was dried under vacuum at 50 °C for 6–7 h. The dried mandelic acid was dissolved in dry THF (25 ml) and added dropwise into a pre-cooled phenyllithium solution (50 ml, 90 mmol plus 50 ml THF) at −70 °C with vigorous stirring under N_2. The reaction mixture was allowed to warm up to room temperature and stirred for 2 h. The solution was then divided into two halves, and each half was poured onto a mixture of NH_4Cl/ice bath (20/150 g) with vigorous stirring. The organic layers were collected and the white precipitates were recovered by filtration and dissolved in CH_2Cl_2. The aqueous layers were further washed with CH_2Cl_2 (2 × 50 ml). All organic solutions were combined and then washed with 5% aqueous $NaHCO_3$ (100 ml), saturated NaCl (100 ml) solution and H_2O (100 ml). The solution was dried by $MgSO_4$ and evaporated under reduced pressure to give a yellowish solid. The solid was washed with hexane and ether to yield **1** (2.79 g, 51%). ^1H NMR ($CDCl_3$) δ 4.57 (d, 1H, J = 6.0 Hz, OH), 5.92 (d, 1H, J = 6.0 Hz, CH), 7.2–7.9 (m, 10H, Ar–H). Lit. [23]: ^1H NMR (DMSO-d_6) δ 6.2 (2 d, AB, CHOH), 7.2–8.1 (m, 10H, Ar–H).

2.3.2. 2-Phenyl-2-(S-α-hydroxybenzyl)-1,3-dioxolane **2**

(*S*)-Benzoin (2 g, 9.43 mmol), ethylene glycol (0.85 ml, 15.27 mmol) and *p*-toluenesulfonic acid (60 mg, 0.32 mmol) were dissolved in dry benzene (60 ml) and refluxed under N_2 for 16 h in a Dean-Stark apparatus. After cooling down, the solution was washed with 5% aqueous $NaHCO_3$ (10 ml) and H_2O (50 ml × 4). The solution was dried by $MgSO_4$ and evaporated under reduced pressure to yield a yellowish residue. Recrystallization from benzene and hexane gave **2** (1.01 g, 42%). ^1H NMR ($CDCl_3$) δ 2.8 (d, 1H, OH), 3.8–4.1 (m, 4H, CH_2), 4.85 (d, 1H, CH), 7.1–7.35 (10H, m, Ar–H). Lit. [23]: ^1H NMR (DMSO-d_6) δ 3.6–4.0 (m, 4H, CH_2), 4.78 (d, 1H, CH), 5.44 (d, 1H, OH), 7.14-7.20 (2 s, 10H, Ar–H).

2.3.3. (2S)-Hydroxy-1,2-diphenylethan[1-^{18}O]one **3**

The dioxolane (**2**) (1.0 g, 3.9 mmol) and anhydrous *p*-toluenesulfonic acid (80 mg, 0.46 mmol) in 1 ml dry dioxane were septum-sealed in a pear-shaped flask. The $H_2{}^{18}O$ (0.8 ml) was added via syringe into the flask. Then, the reaction mixture was heated at 90 °C for 3.5 h under nitrogen. After 3.5 h, the dioxane–water mixture was recovered for re-use through a vacuum line. The solid residue was dissolved in CH_2Cl_2 (40 ml) and washed with 5% aqueous $NaHCO_3$ (10 ml) and H_2O (2 × 30 ml). The organic layer was then dried by anhydrous $MgSO_4$ and evaporated to give a white solid. Recrystallization from benzene and hexane yielded **3** (548 mg, 66%). ^1H NMR ($CDCl_3$) δ 4.57 (d, 1H, J = 6.0 Hz, OH), 5.92 (d, 1H, J = 6.0 Hz, CH), 7.2–7.9 (m, 10H, Ar–H); IR (cm^{-1}): 1650.6 (C=^{18}O) [1681 for C=^{16}O]. Lit. [23]: not previously reported.

2.3.4. (1R,2S)-1,2-[1-^{18}O]Dihydroxy-1,2-diphenylethane **4**

In a glove box, solid $NaBH_4$ (113 mg, 2.8 mmol) was added in portions to a suspension of ^{18}O-benzoin (**3**, 0.6 g, 2.8 mmol) in dry ethanol (9 ml). The solution was stirred at 50 °C for 10 min. Outside the glove box, addition of water (36 ml) to the reaction mixture gave a white precipitate. The precipitate was washed with ether and hexane to yield pure ^{18}O-*meso*-hydrobenzoin (**4**, 256 mg, 43%). ^1H NMR ($CDCl_3$) δ 4.77 (s, 2H, CH), 2.09 (s, 2H, OH), 7.0–7.4 (m, 10H, Ar–H). Lit. (for ^{16}O-*meso*-hydrobenzoin) [23]: ^1H NMR ($CDCl_3$) δ 4.78 (s, 2H, CH), 2.78 (s, 2H, OH), 7.2 (s, 10H, Ar–H).

2.3.5. Phosphorus [^{17}O]oxychloride

$H_2{}^{17}O$ (100 μl, 5.55 mmol) was added dropwise to pre-cooled solid PCl_5 (1.315 g, 6.31 mmol) while stirring. The solution was allowed to warm up to room temperature and then heated at 98 °C

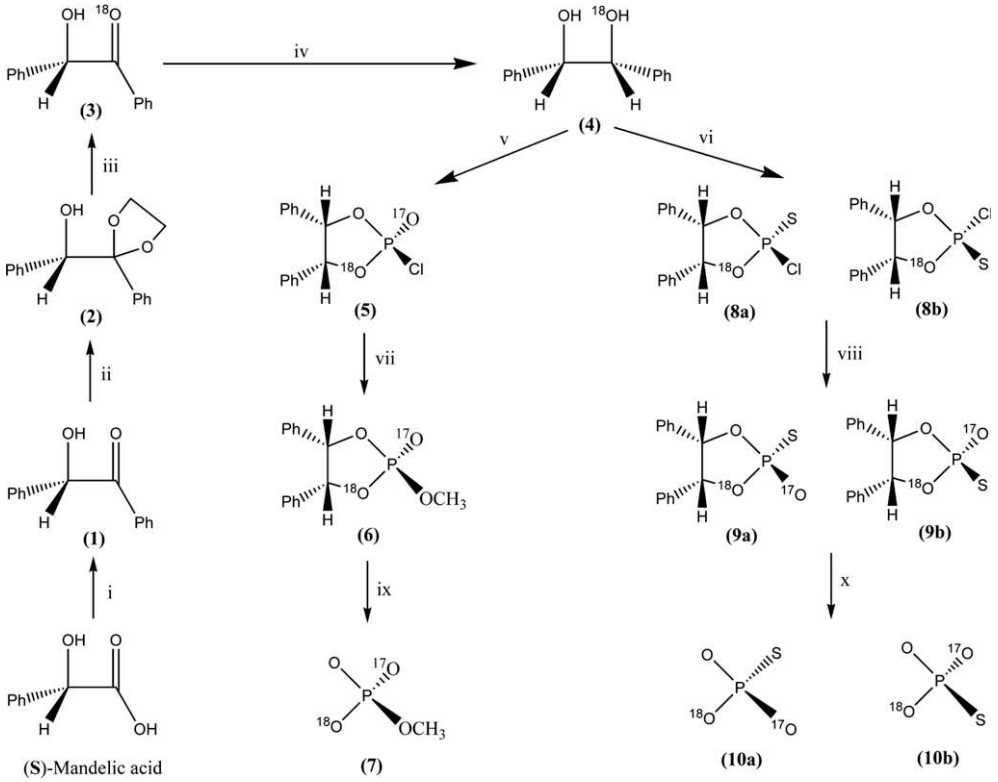

Scheme 1. (i): PhLi in THF; (ii): $HO(CH_2)_2OH$, *p*-$MeC_6H_4SO_3H$ in benzene; (iii): $H_2{}^{18}O$, *p*-$MeC_6H_4SO_3H$ in dioxane; (iv): $NaBH_4$ in ethanol; (v): $P^{17}OCl_3$ in pyridine; (vi): $PSCl_3$ in pyridine; (vii): MeOH in pyridine; (viii): $H_2{}^{17}O$ in pyridine; (ix): H_2, Pd/C in ethyl acetate; (x): Na in liquid NH_3.

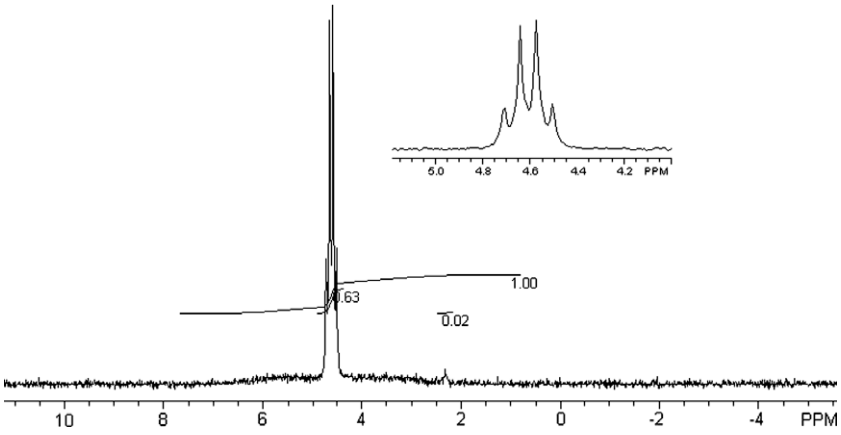

Fig. 3. ^{31}P NMR (D_2O) of **7**. δ_P 4.6 (*q*, $^3J_{PH}$ = 9.5 Hz, $MePi^*$), 2.3 (s, Pi). The inset enlarges the quartet at δ_P 4.6.

for 30 min before being distilled to yield a clear liquid (425 μl, 78%). ^{31}P NMR (neat) δ 2.95 (m). Lit. [23]: not previously reported.

2.3.6. (2R,4S,5R)-2-Methoxy-2-[^{17}O]oxo-4,5-diphenyl-[1-^{18}O]-1,3,2-dioxa-phospholane **6**

^{18}O-labeled diol (**4**, 150 mg, 0.69 mmol) in dry pyridine (2.66 ml) was added to a solution of $P^{17}OCl_3$ (64 μl, 0.71 mmol in 1.9 ml pyridine) at 0 °C over a period of 2 h with vigorous stirring. After further stirring at room temperature for 30 min, the solution was cooled back to 0 °C. Anhydrous methanol (30 μl, 0.71 mmol in 0.72 ml pyridine) was added to the pre-cooled mixture over 20 min with vigorous stirring. After being stirred for 1 h, the solvent was removed under reduced pressure and the residue was partitioned between cold benzene (30 ml) and water (6 ml). The benzene layer was washed with cold $NaHCO_3$ (5%, 10 ml) and cold water (2 × 15 ml) and dried by $MgSO_4$. Evaporation of benzene yielded a yellowish solid (150 mg, 74%). ^{31}P NMR ($CDCl_3$) δ 14.05 (m); ^1H NMR ($CDCl_3$) δ 3.84 (d, 3H, $^3J_{HP}$ = 11.7 Hz, Me), 5.69 (d, 2H, $^3J_{HP}$ = 8.3 Hz, CH), 6.8–7.2 (m, 10H, Ar–H). Lit. [23]: ^{31}P NMR ($CHCl_3$, D_2O lock) δ 13.4; ^1H NMR ($CDCl_3$) δ 3.95 (d, 3H, $^3J_{HP}$ = 11.7 Hz, Me), 5.78 (d, 2H, $^3J_{HP}$ = 8.3 Hz, CH), 6.9–7.5 (m, 10H, Ar–H).

2.3.7. Methyl (S)-[^{16}O, ^{17}O, ^{18}O]-phosphate (disodium salt) **7**

Dioxaphospholane (**6**, 150 mg, 0.51 mmol) and catalyst (Pd–C; 50 mg, 10 wt%, dried over drierite in a vacuum desiccator) were mixed in ethyl acetate (6 ml) and vigorously stirred for 2 h at room temperature under H_2. After 2 h, the catalyst was filtered off and

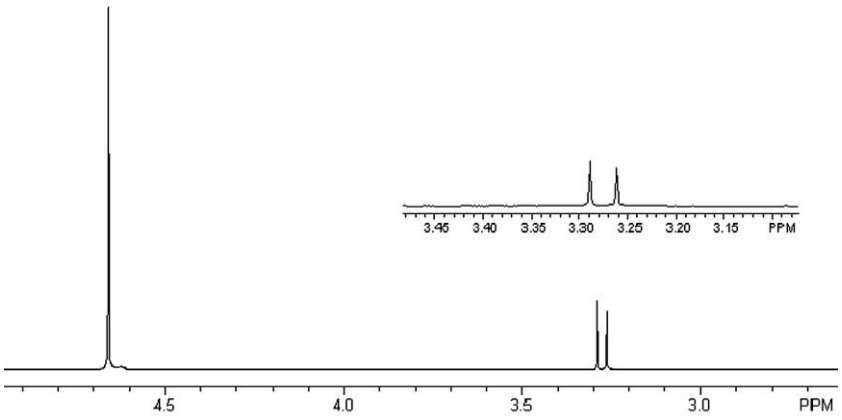

Fig. 4. ^{1}H NMR (D_2O) of **7**. δ_H 3.3 (d, $^{3}J_{HP}$ = 9.9 Hz, Me), 4.66 (s, HOD). The inset enlarges the doublet at δ_H 3.3.

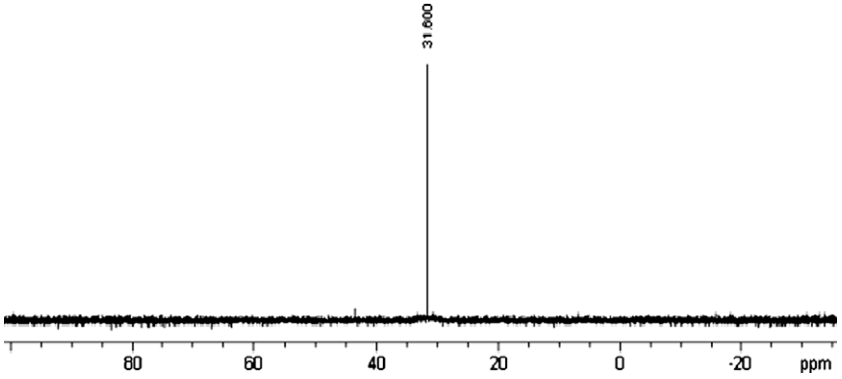

Fig. 5. ^{31}P NMR of (*R*)-TPi*.

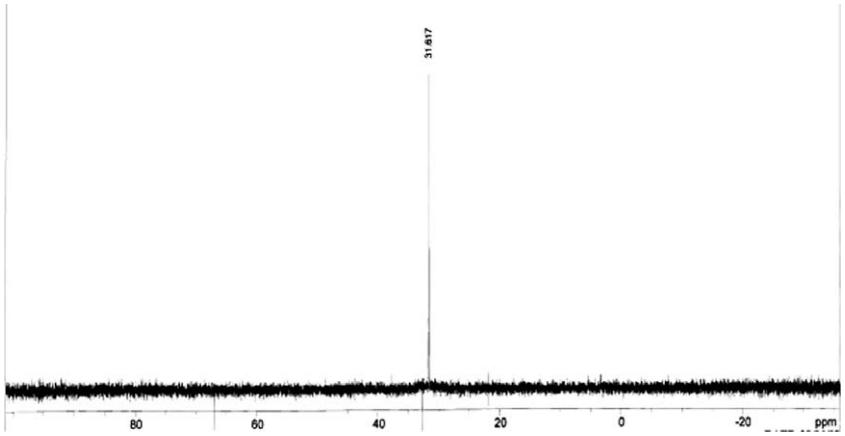

Fig. 6. ^{31}P NMR of (*S*)-TPi*.

washed with hot ethyl acetate (3 × 15 ml). Evaporation of ethyl acetate by vacuum gave a clear gum. The gum was partitioned between water (25 ml) and ether (15 ml). The aqueous layer was further washed with ether (3 × 15 ml) and then adjusted by NaOH solution to pH 8.12. The solvent was removed to yield a white powder (66 mg, 62%). ^{31}P NMR (D_2O) δ 4.6 (q, $^{3}J_{PH}$ = 10.2 Hz); ^{1}H NMR (D_2O) δ 3.3 (d, 3H, $^{3}J_{HP}$ = 10.2 Hz, Me); ^{17}O NMR (H_2O, 92 °C) δ 100.4 (d, $^{1}J_{OP}$ = 103.4 Hz); MS (FAB) *m*/*z* calcd for CH_3O-PO_3H $(M^{2-}+H^{+})^{-}$ 114. Found 114. Lit. (for unlabeled **7**) [23]: ^{31}P NMR (D_2O) δ 1.9; ^{1}H NMR (D_2O) δ 3.5 (d, 3H, $^{3}J_{HP}$ = 11.8 Hz, Me).

*2.3.8. Cis- and trans-(4R,5S)-4,5-Diphenyl-1,3,2-[1-^{18}O]dioxaphospholane-2-thiol- 2-[^{17}O]one **9a** and **9b***

^{18}O-diol **4** (215.2 mg, 1 mmol) was dried by coevaporation with dry pyridine (3 × 4ml), and then dissolved in dry pyridine (6 ml). The resulting solution was slowly added to $PSCl_3$ (300 μl, 3 mmol) in 6 ml dry pyridine at 50 °C over 2 h. After another 2 h of stirring, $H_2{}^{17}O$ (125 μl, 7 mmol) in dry pyridine (2 ml) was added dropwise over 30 min, and stirring continued for another 10 min. The pyridinium hydrochloride salt was filtered off after the reaction solution cooled down. The solvent was removed under reduced pressure

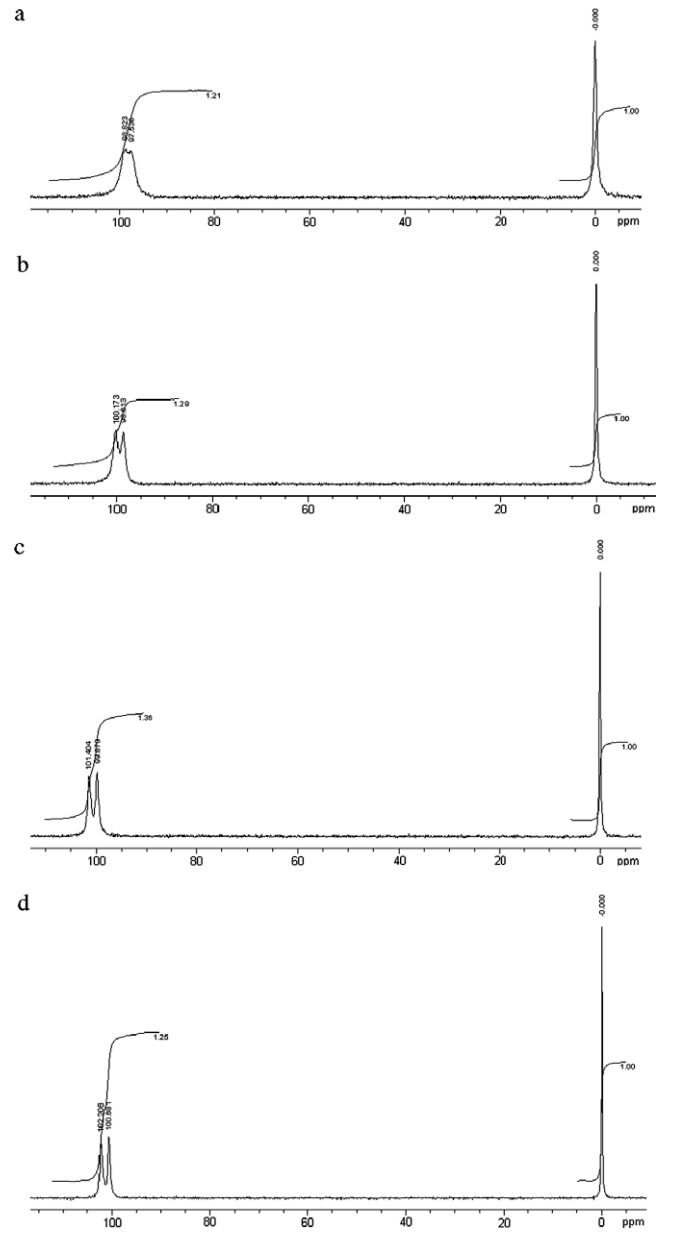

Fig. 7. ^{17}O-NMR spectra of **7** at: (a) ~300 K, δ^{17}O: 0.0, $H_2{}^{17}O$; 98.18, (d, ^{17}O–MePi, $^1J_{OP}$ = 87.3 Hz); (b) at 320 K, δ^{17}O: 0.0, $H_2{}^{17}O$; 99.39 (d, ^{17}O–MePi, $^1J_{OP}$ = 105.7 Hz); (c) at 345 K, δ^{17}O: 0.0, $H_2{}^{17}O$; 100.14 (d, ^{17}O–MePi, $^1J_{OP}$ = 104 Hz); (d) at 365 K, δ^{17}O: 0.0, $H_2{}^{17}O$; 100.44 (d, ^{17}O–MePi, J_{OP} = 103.4 Hz).

and the residue was partitioned between H_2O (20 ml) and CH_2Cl_2 (20 ml). The aqueous layer was extracted with CH_2Cl_2 (20 ml). The organic layers were then combined and the solvent was removed under reduced pressure. The residue was converted into a sodium salt (255.1 mg, 0.81 mmol) and then separated on a semi-prep C18 column (mobile phase: 30% CH_3CN, 10% MeOH and 60% 50 mM triethylammonium bicarbonate at pH 7.2). The *trans* isomer, **9b**, (37.4 mg, 0.096 mmol, 9.6%) was eluted first followed by the *cis* isomer, **9a**, (136.3 mg, 0.35 mmol, 35%). ^{31}P NMR (MeOH) δ 73.41 (t, $^3J_{PH}$ = 7.0 Hz, *cis*), 70.56 (t, $^3J_{PH}$ = 8.2 Hz, *trans*). Lit. [23]: ^{31}P NMR (MeOH-d_4) δ 69.1 (*cis*), 66.5 (*trans*); ^{17}O NMR (MeOH, D_2O lock) δ 144 (±8 ppm, *cis*), 138 (±8 ppm, *trans*).

2.3.9. (R)-[^{16}O, ^{17}O, ^{18}O]Thiophosphate (trisodium salt) ***10a***

Compound **9a** (136.3 mg, 0.35 mmol) was dissolved in dry liquid NH_3 (~20 ml, freshly distilled from NH_4OH solution and redistilled again from Na metal) at −78 °C. Excess Na metal was added to the solution until a dark blue color was seen. After 30 min stirring, excess EtOH (~3 ml) was added to quench the reaction. NH_3 was evaporated under a stream of N_2 gas while the mixture warmed up to room temperature. The solvent was removed under reduced pressure and the product was extracted with water. The water was then removed under reduced pressure and the residue washed with EtOH several times to give the pure product. ^{31}P NMR (H_2O) δ 31.60. MS (FAB) *m*/*z* calcd for SPO_3NaH $(M^{3-}+Na^+ + H^+)^-$ 137.9. Found 138. Lit. (for bis-triethylammonium salt) [23]: ^{31}P NMR (MeOH-d_4) δ 45 (bs).

2.3.10. (S)-[^{16}O, ^{17}O, ^{18}O]Thiophosphate (trisodium salt) ***10b***

Compound **9b** (37.4 mg, 0.096 mmol) was treated by the same procedure to give **10b**. ^{31}P NMR (H_2O) δ 31.62. MS (FAB) *m*/*z* calcd for SPO_3NaH $(M^{3-}+Na^+ + H^+)^-$ 137.9. Found 138. Lit. (for bis-triethylammonium salt) [23]: ^{31}P NMR (MeOH-d_4) δ 45 (bs).

2.4. Theoretical calculations

TDDFT ECD calculations were performed at the B3LYP/6-311G** level using GAUSSIAN 03 [22]. Anharmonic frequency calculations were first carried out using GAUSSIAN 03 to predict the isotopically-perturbed geometries of MePi* and TPi*. Electronic rotational strengths, oscillator strengths and excitation energies were then calculated using these perturbed geometries. In the case of TPi*, calculations were also carried out for a hydrated complex, $(TPi^*)(H_2O)_6$.

3. Results and discussion

3.1. Synthesis

The synthesis of MePi* and TPi* followed the original work of Lowe et al. [18,23] (Scheme 1) with minor but advantageous modifications, such as the use of HPLC to isolate the products.

The synthesis began with reaction of (*S*)-mandelic acid and phenyllithium to make (*S*)-benzoin, **1**. (*S*)-Benzoin was then converted to its acetal form (**2**) with ethylene glycol via acid catalysis, and ^{18}O introduced by hydrolysis with $H_2{}^{18}O$ to yield ^{18}O-labeled (*S*)-benzoin, **3**, which we confirmed by the lower frequency shift of the C=^{18}O stretching band (1651 cm^{-1}) from the C=^{16}O stretching band (1681 cm^{-1}) using IR spectroscopy. Reduction of ^{18}O-labeled (*S*)-benzoin by sodium borohydride then gave the ^{18}O-labeled diol, **4**. Thereafter, the synthesis differs between MePi* and TPi*.

For MePi*, ^{18}O-labeled diol was treated with phosphorus [^{17}O]oxychloride in pyridine to form exclusively *trans*-[1-^{18}O, 2-^{17}O]-2-chloro-dioxaphospholane, **5**. Methanolysis of **5** proceeded with retention of configuration [20], thus giving *trans*-[1-^{18}O, 2-^{17}O]-2-methoxy-dioxaphospholane, **6**, predominantly. Compound **6** was then reductively cleaved by hydrogen on Pd/C to give methyl (*S*)-[^{16}O, ^{17}O, ^{18}O]-phosphate, **7**. Some inorganic phosphate was also produced during the hydrogenolysis, as seen from ^{31}P NMR, possibly due to traces of moisture. We then purified the target compound by washing with acetone and extraction into methanol, reducing the inorganic phosphate content to <5%, as evidenced from the ^{31}P NMR integration. The ^{31}P and ^{1}H NMR spectra of **7** are displayed in Figs. 3 and 4. The broad bumps at the base of the major peak provide evidence of ^{17}O, due to the quadrupolar nature of the ^{17}O nucleus.

As for TPi*, the ^{18}O-labeled diol **4** was treated with thiophosphoryl chloride in pyridine to form both *cis*- and *trans*-[1-^{18}O]-2-chloro-thiol-dioxaphospholane (**8a** and **b**), with the *cis* to *trans* ratio ca. 3:1 (^{31}P NMR integration). The mixture of diastereoisomers

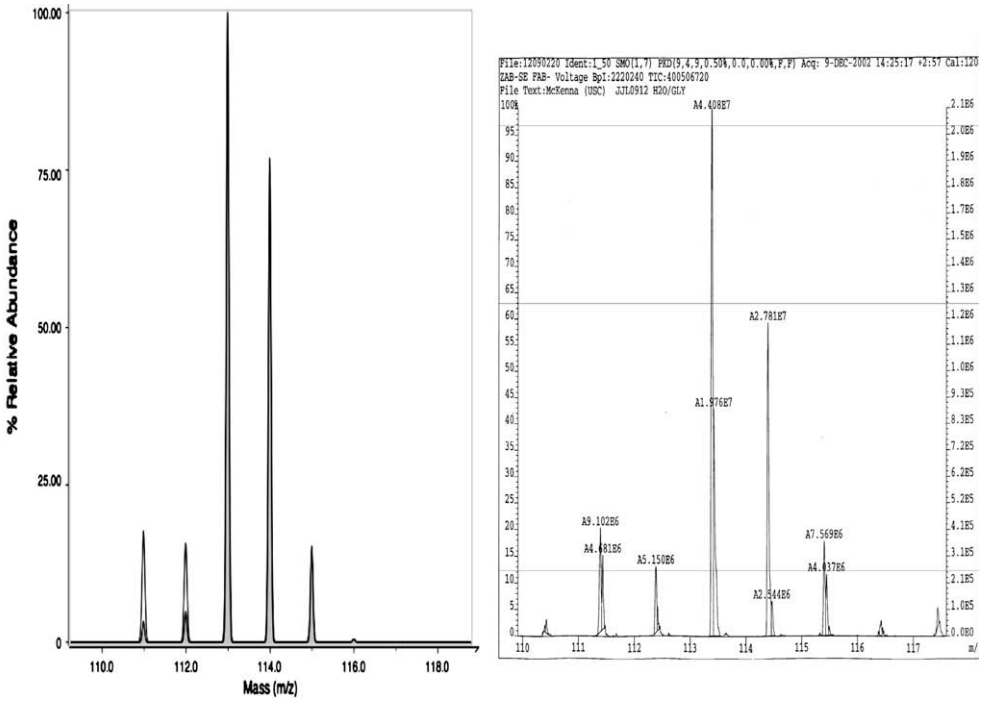

Fig. 8. Comparison of predicted (left) and experimental (right) mass spectra of **7**. Experimental *m*/*z* offset, +0.5. Solid predicted spectrum calculated based on assumed initial oxygen isotope contents of $H_2{}^{17}O$ and $H_2{}^{18}O$-enriched starting reagents; hollow predicted spectrum, after fitting to experimental data by partial loss of heavy oxygen isotope (see text).

of **8** was hydrolyzed by $H_2{}^{17}O$ to give *cis*- and *trans*-[1-^{18}O, 2-^{17}O]-thiol-dioxaphospholane, **9a** and **9b**, with a *cis* to *trans* ratio ca. 3:1. We found that the ratio of the **9** diastereoisomers varied with the reaction temperature, i.e., as the hydrolytic temperature was lowered, the ratio approached that for **8**, indicating that the hydrolysis did not necessarily proceed with retention of configuration. The diastereoisomers of **9** were separated on a semi-preparative reverse phase C18 column. The modern HPLC column provided much better reproducibility than conventionally self-packed columns [18], which proved especially valuable since all conditions were refined on the unlabeled compounds before being applied to the expensive labeled ones. Lastly, reductive cleavage of **9** was carried out with sodium in liquid ammonia to give the target (*R*) and (*S*) enantiomers of **10**. ^{31}P NMR spectra of (*R*)-**10** and (*S*)-**10** are shown in Figs. 5 and 6. Again, the broad bumps around the base of the peaks show ^{17}O labeling.

3.2. Stereochemical characterization of MePi* and TPi*

3.2.1. General considerations

The MePi* and TPi* enantiomers have undetectable optical rotations, and are not readily analyzed by routine methods such as chiral HPLC. The evidence for stereospecific formation of the intermediate phospholane **6** has been discussed in detail by Lowe [13]. The final step, hydrogenation of **6**, is considered to proceed with retention, giving **7**. When ^{17}O is introduced into precursor **5**, the % isotopic enrichment in the $H_2{}^{17}O$ should be sustained through formation of **7**; decrease in ^{17}O (or ^{18}O) content by hydrolytic exchange (or inadvertent dilution of heavy oxygen in a labeling reagent) should correspond to decreased %ee in the final product, by producing an achiral methyl phosphate. Equivalent exchange of the unesterified oxygens in the chiral product would lead to 1:1 dilution:exchange if the ^{17}O or ^{18}O label were replaced by adventitious ^{16}O regardless of mechanism, whereas replacement of an original ^{16}O could result in no effect (retention), 2:1 dilution: exchange (inversion) or 1:1 dilution:av. exchange (racemization). From this, it follows that the overall dilution for random oxygen replacement will have a minimum effect of 2/3 dilution per exchange (with retention), and a maximum effect of 4/3 dilution per exchange (with an inversion); absent information about the mechanism, a % loss of positional labels should correspond directly to a proportional % loss of ee with an uncertainty of ±1/3.

For TPi*, the precursors **9a** and **9b** are diastereomers separable by chromatography and their cleavage to the individual TPi* enantiomers by Na/NH_3 should proceed with retention [18]. NMR analysis of the stereoisomers generated in the indirect chemical method presented in Ref. [18] was done by adjusting the data to a predicted spectrum taking into account actual % enrichments in the heavy oxygen isotopes, using loss of label and possible racemization as fitting factors, however the data and analysis were not presented [20]. Finally, because the available $H_2{}^{17}O$ and $H_2{}^{18}O$ are not isotopically pure, formation of the opposite enantiomers must be considered. From the starting percentages of ^{17}O in the $H_2{}^{17}O$ (40.2%), and ^{18}O in the $H_2{}^{18}O$ (94.6%), we obtain an upper limit of 38.0% ee for the synthesized enantiomers. The contaminating heavy oxygen in the respective samples (7.4%, 2.2%) will result in <0.2% of the opposite enantiomer, so this correction is negligible.

3.2.2. ^{17}O NMR of MePi*

Since the isotopically chiral compounds contain, besides ^{31}P, another NMR active nucleus, ^{17}O, we decided to first verify the presence of this label by ^{17}O NMR. Although ^{17}O NMR has been applied widely in both chemical [24] and biochemical studies [25], it has significant limitations. Firstly, the natural abundance of ^{17}O is quite low (0.037%). Secondly, the quadrupolar nature of ^{17}O (I = 5/2) tends to broaden the signals and high temperatures are needed to reduce resonance linewidths [26].

Several singly ^{17}O-labeled phosphate and thiophosphate derivatives have been reported by Gerlt et al., including monomethyl [^{17}O]-phosphate and [^{17}O]-thiophosphate [26,27], which provide

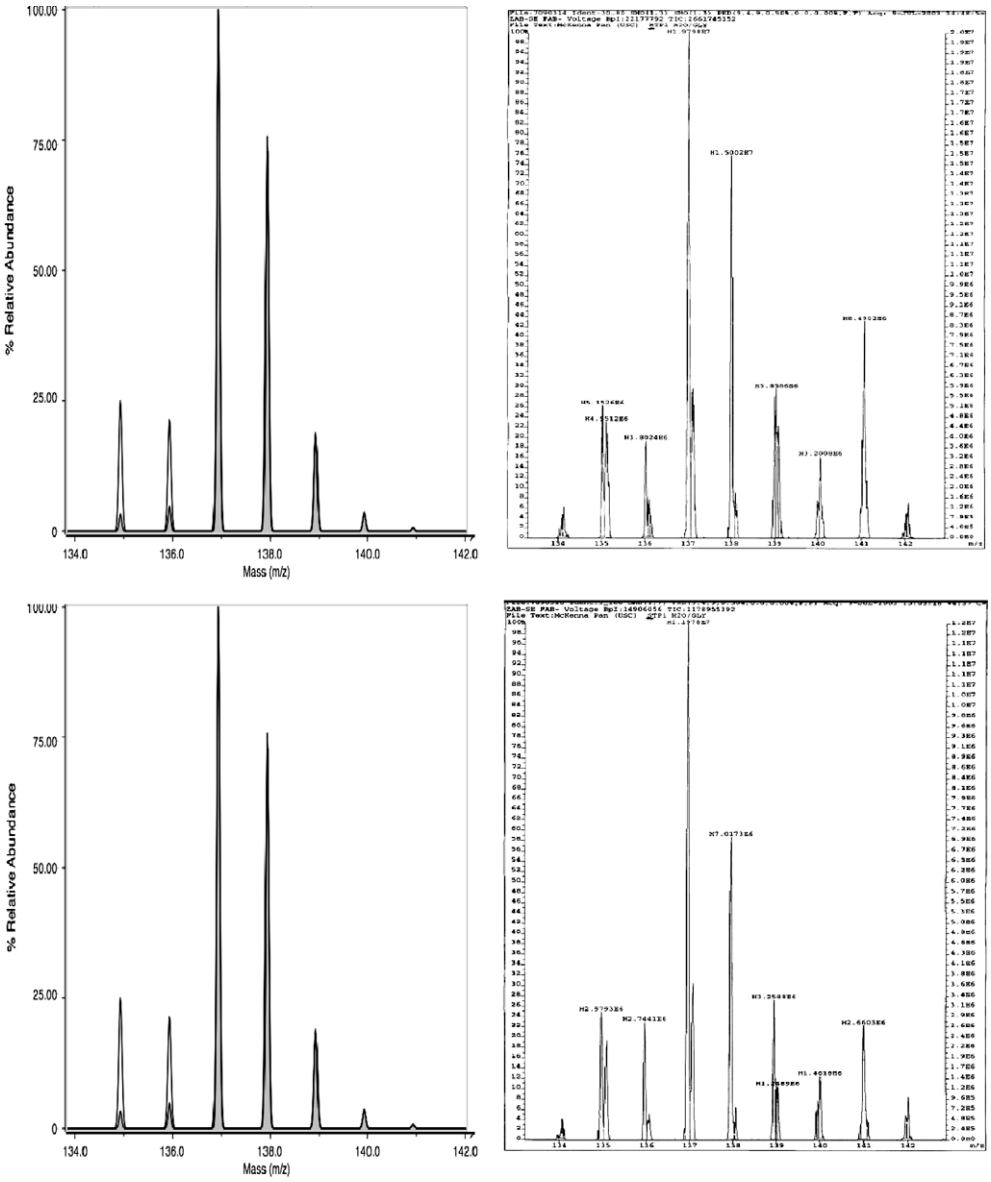

Fig. 9. Comparison of predicted (left) and experimental (right) mass spectra of **10** enantiomers. Top: (*R*)-isomer, **10a**; bottom: (*S*)-isomer, **10b**. Solid predicted spectra calculated based on assumed initial oxygen isotope contents of $H_2{}^{17}O$ and $H_2{}^{18}O$-enriched starting reagents; hollow predicted spectrum, after fitting to experimental data by partial loss of heavy oxygen isotope (see text). Peaks at *m*/*z* 140–142 attributed to system background (*m*/*z* 140, partially).

good references for our compounds. ^{17}O NMR data for (*R*)-TPi* and (*S*)-TPi* have also been reported by Lowe et al., presumably at room temperature, showing very broad linewidths [18].

The ^{17}O NMR spectra of **7** at different temperatures are shown in Fig. 7a–d. As anticipated, the linewidths of both **7** and $H_2{}^{17}O$ decrease as the temperature increases, leading to an increasingly well-resolved ^{17}O–^{31}P coupling doublet. ^{17}O NMR data for MePi* were not reported by Lowe et al. [23]. We therefore compared our results with those for [^{17}O, ^{16}O, ^{16}O]-MePi reported by Gerlt et al. [26]. The chemical shift of our MePi* sample was δ_O 100.4 ppm with $^1J_{OP}$ = 103.4 Hz at 92 °C, while they obtained δ_O 101.7 ppm and $^1J_{OP}$ = 104 Hz at 95 °C. The values are in good agreement, allowing for differences in the sample pH and concentration. The concentration of the ^{17}O-labeled MePi can be estimated from the spectra. Based on the concentration of neat water (55 M) and the natural abundance of ^{17}O (0.037%), the concentration of $H_2{}^{17}O$ was calculated to be 0.020 M. From integration of the ^{17}O NMR peaks, the concentration of ^{17}O-labeled MePi is ~0.025 M, or 42% of the total methyl phosphate concentration (0.06 M). This result is consistent with the value of 40.2% ^{17}O provided for the ^{17}O-water used in our synthesis, when 2% is deducted for ^{17}O contributed by the ^{18}O-water used (however, the error of the determination will somewhat exceed this value).

A temperature-dependent study of ^{17}O NMR of TPi* was not carried out because of its extremely rapid hydrolysis at the raised temperatures needed to achieve narrow signal linewidths [26]. However, the presence of ^{17}O in the samples is qualitatively confirmed by the quadrupole broadening evident in their ^{31}P NMR spectra at room temperature (Figs. 5 and 6).

3.2.3. Mass spectroscopy

MS analysis of MePi* or TPi* samples allows a determination of the relative isotopomer content in these compounds, making possible an estimate of stereopurity (see above). The FAB mass spectra of the three labeled compounds, **7**, **10a** and **10b**, were recorded and compared to the theoretically calculated ones, based

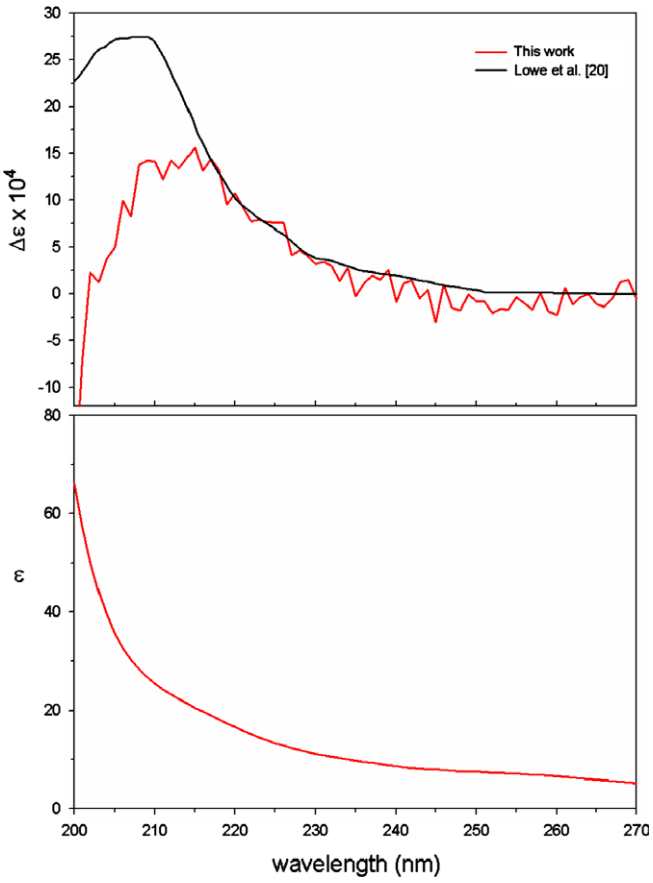

Fig. 10. UV and ECD spectra of MePi*. The ECD spectra are normalized to 100% ee. Lower ECD and UV: this work (disodium salt, 0.047 M in H_2O, pH 8). Upper ECD spectrum: reproduced from Cullis and Lowe (disodium salt, 0.03 M in D_2O) [20]).

on the possible isotopic combinations arising from the isotopic oxygens in the $H_2{}^{17}O$ and $H_2{}^{18}O$, together with a 4% contribution from ^{34}S in **10** and negligible contributions from the other naturally abundant oxygen, carbon and sulfur isotopes.

Inspection of the experimental mass spectrum for **7** in comparison with its predicted spectrum based on the nominal isotope content of the starting $H_2{}^{17}O$ and $H_2{}^{18}O$ shows that the expected pattern is present, but a minor loss of heavy oxygen isotope is apparent (Fig. 8). A stepwise replacement with ^{16}O at the ^{17}O-labeled position did not improve the fit, but replacement at the ^{18}O-labeled position gave an excellent fit assuming a fitting parameter of 12.5% exchange (Fig. 8; for details of the calculations, see Supplementary material), corresponding to an estimated %ee of 33%, vs. 38% for the unadjusted isotopic oxygen composition of **7**.

A similar picture is presented for the two **10** enantiomers. Again the overall patterns in the experimental and predicted spectra are similar for both **10a** and **10b**, but some loss of heavy oxygen isotope is also evident (Fig. 9). Of various possible oxygen exchange schemes, the best fit for both experimental spectra was found to result with exchange at the ^{18}O-labeled position (18%), corresponding to an estimated %ee of 31% (both isomers), vs. 38% without loss of label.

3.3. ECD results

3.3.1. Spectroscopy of MePi*

The UV absorption and ECD spectra of the disodium salt of **7** over the wavelength range 200–270 nm are shown in Fig. 10. The concentration, determined using ^{31}P NMR, was 0.047 M. The ECD spectrum is normalized to 100% ee, using 33% estimated from the MS data fit. The normalized ECD spectrum exhibits a weak, broad peak with positive CD at ~210 nm, with a less than ideal signal-to-noise ratio and with an anisotropy ratio of $\sim 4.5 \times 10^{-5}$. The ECD spectrum reported by Cullis and Lowe [20], also normalized to 100% ee, is included in Fig. 10 for comparison. This spectrum exhibits a peak at 208 nm whose magnitude is approximately twice that of our ECD spectrum, however the actual S/N of their spectrum, obtained with an earlier generation CD instrument, is not apparent.

3.3.2. Spectroscopy of TPi*

Unlike MePi, TPi has prominent, well-defined peaks in its UV spectrum which are pH dependent, with λ_{max} at 208, 225 and 238 nm at pH 0.5–5.0, 5.5–10 and 11–13, respectively [28,29]. H_3PO_3S and $H_2PO_3S^-$ predominate at 0.5–5.0, HPO_3S^{2-} at 5.5–10, and PO_3S^{3-} at 11–13. We first verified the UV spectral properties of unlabeled TPi in the pH range of 12.42–4.46, confirming two obvious isosbestic points in this range, corresponding to the equilibria between PO_3S^{3-} and HPO_3S^{2-}, and between HPO_3S^{2-} and $H_2PO_3S^-$ (Supplementary material). The absorption spectrum is unchanged above pH 12.0, with a maximum at 236 nm and is also essentially invariable between pH 7.0 and 9.0, with a maximum at 224–5 nm. The pK_{a2} and pK_{a3} were estimated as 5.2–5.8 and 11.0–11.2, and extinction coefficients (ε) at 224–5 nm and 236 nm were estimated to be 3990 and 3779, which may be compared to the literature values, ε 3736 at 225 nm and 3630 at 238 nm [28].

The pH dependence of the stability of TPi has also been previously studied [29]. The relative stability of different species of TPi is $PO_3S^{3-} > H_3PO_3S > HPO_3S^{2-} > H_2PO_3S^-$. Both PO_3S^{3-} and

Table 1
Experimental and calculated ECD comparison of MePi* (**7**) and TPi* (**10a, b**).

	Expt			B3LYP/6-311G**//B3LYP/6-311G**			
	pH	$\lambda_{excitation}$[a]	$\Delta\varepsilon/\varepsilon$[b]	$\lambda_{excitation}$[a]	R[c]	f[d]	$\Delta\varepsilon/\varepsilon$[e]
$CH_3OPO_3^{2-}$	8.0	<190	4.5×10^{-5}	337.12	0.0033	0.0002	
				337.10	−0.0009	0.0002	2.9×10^{-5}
				337.12	0.0007	0.0002	
$HSPO_3^{2-}$	9.0	225	$<5 \times 10^{-6}$				
SPO_3^{3-}	12.0	236	$<5 \times 10^{-6}$	290.89	0.0004	0.0103	-5.3×10^{-6}
				290.89	−0.0088	0.0000	
$SPO_3^{3-} + [6H_2O]$	12.0	236	$<5 \times 10^{-6}$	252.63	−0.0214	0.0441	1.7×10^{-6}
				252.33	0.0426	0.0454	

[a] λ in nm. Estimated at the excitation wavelengths except for $CH_3OPO_3^{2-}$, which is estimated at 208 nm (100% ee).
[b] Exp. %ee values used: 33% for **7**; 31% for **10a,b**.
[c] R values in 10^{-40} esu^2 cm^2.
[d] Oscillator strengths.
[e] Estimated via $4R/D$, where $D = 2.13 \times f \times \lambda$ (nm) $\times 10^{-37}$ esu^2 cm^2. R and f are the sums of the individual excitations with close excitation energies.

HPO_3S^{2-} (pH > 7.6) are fairly stable at room temperature, their stability being enhanced by exclusion of air.

The UV and ECD spectra of the di- and trisodium salts of both enantiomers of TPi* were therefore measured at pH 9 and 12 over the wavelength range 200–270 nm. No significant ECD was detected for either enantiomer at either pH. At the peak wavelengths of the UV absorption bands at 225 nm and 236 nm at pH 9 and 12, respectively, our data yields upper limits to the corresponding ECD anisotropy ratios of 5×10^{-6}.

3.3.3. Calculated ECD for MePi* and TPi*

To evaluate our experimental estimates of the ECD of MePi* and TPi* from a theoretical perspective, we carried out time-dependent DFT (TDDFT) calculations of their electronic excitation energies and rotational strengths, using the functional B3LYP and the basis set 6-311G**. The isotopically-perturbed geometries of MePi* and TPi* were predicted using the anharmonic vibrational frequency calculational code in GAUSSIAN 03. In the case of TPi*, calculations were also carried out for the hexahydrated complex, $(TPi^*)(H_2O)_6$, to investigate the impact of the aqueous solvent. The wavelengths of the lower energy electronic excitations and their oscillator strengths and rotational strengths are given in Table 1. The predicted excitation wavelengths are greater than the observed wavelengths, a not unusual result of TDDFT calculations [30]. The predicted anisotropy ratios are 2.9×10^{-5} for MePi*, -5.3×10^{-6} for TPi*, and 1.7×10^{-6} for $(TPi^*)(H_2O)_6$. For MePi* the predicted anisotropy ratio approximates that observed. For TPi*, the experimental anisotropy ratios are comparable to the predicted magnitude of the value for **10a/b**. The lower predicted value for **10a/b** $\cdot (H_2O)_6$ suggests that the aqueous environment of TPi* does in fact affect its ECD. Altogether, the TDDFT calculations support the conclusion that the experimental ECD results may be reliable in order of magnitude.

4. Conclusion

Our experimental and theoretical studies support the original claim of Cullis and Lowe that the ECD of MePi* is detectable, although our anisotropy ratio of 4.5×10^{-5} is significantly smaller. However, the S/N is much smaller than in their reported ECD spectrum, despite the use of a newer generation spectrometer, and we note that the observed signal represents a small difference between two much larger ones (Supplementary material), therefore it must be regarded as marginal. Although the possibility exists, in principle, that ECD can be used to determine the stereochemistry of phosphoryl-transfer reactions where MePi* is a product, at best, exact quantitations will be difficult. It should be emphasized that in these measurements, the sensitivity and reliability of the CD instrument to be used at wavelengths <250 nm is important, ^{17}O NMR and MS analysis of the labeled intermediates and product should be performed to monitor label retention, and the highest available oxygen isotope enrichments should be utilized. It would also be of interest to verify the ECD of the (*R*) enantiomer of MePi*, as only the (*S*) enantiomer has been investigated.

We were unable to confirm detectable ECD for TPi* in either the trianion or dianion state, and thus the ECD of TPi* certainly cannot be used to determine the stereochemistry of phosphoryl-transfer reactions with existing instrumentation.

Acknowledgments

We thank Mr. Ron New (UCR-RLMS) for assistance in obtaining the mass spectra reported here. This research was supported by grants from the American Chemical Society (to C.E.McK. & P.J.S., ACS-PRF 35548-AC3) and the National Science Foundation (to P.J.S., CHE-0209957 and CHE-0614577). We also thank the USC High Performance Computing and Communication (HPCC) facility for computer time, Hewlett–Packard Inc. for the use of an Alpha Server SC (ES45) HP computer, and Dr. J.R. Cheeseman of Gaussian Inc. for his assistance and advice.

Appendix A. Supplementary material

Methodological details for MS analysis of isotope contents, raw ECD spectra, IR spectrum of **3** and Tables of digitalized data for experimental, unfitted predicted, and fitted predicted MS of **7**, **10a** and **10b**; study of the pH dependence of the UV spectrum of unlabeled TPi. Supplementary data associated with this article can be found, in the online version, at doi:10.1016/j.bioorg.2009.02.001.

References

[1] M.E. DiSanto, Curr. Pharm. Design 11 (2005) 3995–4010.
[2] H.K. Lee, Pharmacol. Therapeut. 112 (2006) 810–832.
[3] C.X. Gong, F. Liu, I. Grundke-Iqbal, K.J. Iqbal, J. Biomed. Biotechnol. (2006) 1–11.
[4] B.D. Gelb, M. Tartaglia, Hum. Mol. Genet. 15 (2006) R220–R226.
[5] A.M. Michie, R. Nakagawa, Hematol. Oncol. 24 (2006) 134–138.
[6] J. Li, G. Gobe, Nephrology 11 (2006) 428–434.
[7] L. Kockeritz, B. Doble, S. Patel, J.R. Woodgett, Curr. Drug Targets 7 (2006) 1377–1388.
[8] B.A. Teicher, Clin. Cancer Res. 12 (2006) 5336–5345.
[9] W.W. Cleland, A.C. Hengge, Chem. Rev. 106 (2006) 3252–3278.
[10] K.N. Allen, D. Dunaway-Mariano, Trends Biochem. Sci. 29 (2004) 495–503.
[11] N.H. Williams, Biochim. Biophys. Acta 1697 (2004) 279–287.
[12] S.L. Buchwald, D.E. Hansen, A. Hassett, J.R. Knowles, Methods Enzymol. 87 (1982) 279–301.
[13] G. Lowe, Acc. Chem. Res. 16 (1983) 244–251.
[14] F. Eckstein, P.J. Romaniuk, B.A. Connolly, Methods Enzymol. 87 (1982) 197–212.
[15] P.A. Frey, Adv. Enzymol. 62 (1989) 119–201.
[16] S.L. Buchwald, J.R. Knowles, J. Am. Chem. Soc. 102 (1980) 6601–6602.
[17] J.R.P. Arnold, G. Lowe, Chem. Soc. Chem. Commun. (1986) 865–867.
[18] J.R.P. Arnold, R.C. Bethell, G. Lowe, Bioorg. Chem. 15 (1987) 250–261.
[19] M.R. Webb, Methods Enzymol. 87 (1982) 301–316.
[20] P.M. Cullis, G. Lowe, J. Chem. Soc., Chem. Commun. (1978) 512–514.
[21] M.D. Tsai, Biochemistry 19 (1980) 5310–5316. This author referred to the ECD observed as "if it is at all real".
[22] Gaussian 03, GAUSSIAN Inc., <www.gaussian.com>.
[23] P.M. Cullis, G. Lowe, J. Chem. Soc., Perkin Trans. I (1981) 2317–2321.
[24] D.W. Boykin (Ed.), ^{17}O NMR Spectroscopy in Organic Chemistry, CRC Press, Boca Raton, FL, 1991.
[25] M.D. Tsai, Methods Enzymol. 87 (1982) 235–279.
[26] J.A. Gerlt, P.C. Demou, S. Mehdi, J. Am. Chem. Soc. 104 (1982) 2848–2856.
[27] J.A. Gerlt, M.A. Reynolds, P.C. Demou, G.L. Kenyon, J. Am. Chem. Soc. 105 (1983) 6469–6474.
[28] D.C. Dittmer, O.B. Ramsay, J. Org. Chem. 28 (1963) 1268–1272.
[29] H. Neumann, I.Z. Steinberg, E. Katchalski, J. Am. Chem. Soc. 87 (1965) 3841–3848.
[30] F. Furche, R. Ahlrichs, C. Wachsmann, E. Weber, A. Sobanski, F. Vögtle, S. Grimme, J. Am. Chem. Soc. 122 (2000) 1717–1724.